ISSN 0304-9892 (Print) ISSN 2455-7463 (Online)
www.vijnanaparishadofindia.org/jnanabha
***Jñānābha*, Vol. 52(2) (2022), 280-290**
(Dedicated to Professor D. S. Hooda on His 80th *Birth Anniversary Celebrations)*

UNSTEADY STAGNATION FLOW OF VISCOELASTIC FLUID THROUGH POROUS MEDIUM OVER STRETCHING/SHRINKING SURFACE USING UCM MODEL

Sushila Choudhary[1], Anil Sharma[2], Prasun Choudhary[3] and Suresh Kumar[4]
[1,2,3]Department of Mathematics, University of Rajasthan, Jaipur-302004, Rajasthan, India
[4]S.B.K. Govt. College, Jaisalmer-345001, Rajasthan, India
Email: sumathru11@gmail.com, anilsharma9414@gmail.com, prasun.iimet@gmail.com
Corresponding author: smusumaths@gmail.com
(Received: December 18, 2021*; In format: December* 18, 2021*; Revised: March* 26, 2022*; Accepted: November* 30, 2022*)*

DOI: https://doi.org/10.58250/jnanabha.2022.52233

Abstract

In the present paper, Upper-Convected Maxwell model is used for formulation of the problem of two-dimensional unsteady stagnation point flow of viscoelastic fluid which passes through a porous medium over a stretching/shrinking surface. The effect of magnetic field on flow is also considered in the presence of time dependent heat source/sink. Using similarity parameters, we convert the governing non-linear system of partial differential equations into non dimensional system of ordinary differential equations. This system of equations is solved by using Runge-Kutta fourth order method with shooting technique. Effect of different physical parameters e.g. Maxwell parameter(β), permeability parameter(K), unsteadiness parameter(γ), velocity ratio parameter(λ) etc. on flow and heat transfer characteristics are analyzed and discussed graphically. It is observed that for some values of λ , dual solution also exists for both velocity and temperature, and existence and uniqueness of solution also depends upon unsteadiness parameter. For the validation of present study, the results are compared to previous investigations and found in good agreement.
2020 Mathematical Sciences Classification: 76A05, 76M55, 76S05, 76W05, 65L06.
Keywords and Phrases: Upper-Convected Maxwell fluid, Unsteady, MHD, Permeability parameter, Heat source/sink, Skin friction coefficient, Nusselt number.

1. Introduction

Non-Newtonian fluids have vast applications in engineering field and industries. Stagnation fluid flow is mostly used in polymer and composite engineering. Flow over stretching/shrinking sheet has applications in many industrial processes, such as manufacture and extraction of polymer and rubber sheets, paper production, wire drawing and glass fiber production. Most of the fluids, used for industrial purposes, are non-Newtonian in their characteristics. For example, multiphase mixtures such as paints, synthetic lubricants, water emulsions etc. Also, there are biological fluids such as saliva, blood at low shear rate, synovial fluid etc., which are non-Newtonian. Foodstuffs such as jams, jellies, soups, etc. are examples of non-Newtonian fluids. Due to the large variety of the non-Newtonian fluids, many models of non-Newtonian fluids exist. Maxwell model is one of them. In this model, relaxation time effect is considered. This fluid model is useful for polymers of low molecular weight. Many researchers have been worked with this model in the presence of different physical conditions.

Crane [4] studied the flow past a stretching plate. Wang [17] investigated flow characteristics of liquid film on an unsteady stretching surface. Mahapatra and Gupta [7] have analyzed heat transfer in stagnation-point flow towards a stretching sheet. Nazar et al. [11] have investigated the unsteady boundary layer flow in the region of the stagnation point on the stretching sheet. Sadeghy et al. [13] have considered the stagnation-point flow of upper-convected Maxwell fluids. Sajid et al. [14] have studied unsteady flow and heat transfer of a second-grade fluid over a stretching sheet. Bhattacharyya [2] have depicted the dual solutions in unsteady stagnation-point flow over a shrinking sheet. Hayat et al. [5] have analyzed the effects of mass transfer on the stagnation point flow of an upper-convected Maxwell (UCM) fluid. Heat transfer analysis of the unsteady flow of a Maxwell fluid over a stretching surface in the presence of a heat source/sink has been performed by Mukhopadhyay [9]. Mukhopadhyay and Bhattacharyya [8] have studied the unsteady flow of a Maxwell fluid over a stretching surface in presence of chemical reaction. Chen et al. [3] have investigated the unsteady MHD stagnation-point flow toward a shrinking sheet with thermal radiation and slip effects. Ramesh et al. [12] have studied the stagnation point flow of Maxwell fluid towards a permeable surface in the presence of nanoparticles. Madhua et al. [6] have considered the unsteady flow of a Maxwell nanofluid over a

stretching surface in the presence of magnetohydrodynamic and thermal radiation effects. Shahid [15] have carried out a numerical study on effectiveness of mass transfer in the MHD Upper-Convected Maxwell fluid flow on a stretched porous sheet near stagnation point. Zaidi and Mohyud-Din [19] analyzed the effects of joule heating and MHD in the presence of convective boundary condition for upper convected Maxwell fluid through wall jet. Na et al. [10] have considered Maxwell fluid flow between vertical plates with damped shear and thermal flux under the effect of free convection. Forced convective Maxwell fluid flow through rotating disk under the thermophoretic particles motion is investigated by Shehzad et al. [16]. Anwar et al. [1] have studied the influence of ramped wall temperature and ramped wall velocity on unsteady magnetohydrodynamic convective Maxwell fluid flow.

In previous studies no one investigate unsteady stagnation point flow and heat transfer for Upper-Convected Maxwell fluid through porous medium as our best knowledge. In present study we consider Upper-Convected Maxwell model to formulate problem of unsteady stagnation point flow of viscoelastic fluid through a porous medium over a stretching/shrinking surface. Besides it, we also consider magnetic effect in the presence of time dependent heat source/sink. A numerical method named Runge-Kutta fourth order method is applied to solve the system of differential equations with the help of shooting technique.

2. Mathematical Analysis

Consider two dimensional unsteady stagnation point flow of viscoelastic incompressible fluid through porous medium over stretching/shrinking surface. The x and y axes are chosen along and perpendicular to the surface, respectively. Surface is stretched or shrunk in its own plane with velocity $u_w(x,t) = \dfrac{bx}{(1-\zeta t)}$, where b is the stretching/shrinking rate with dimension $(time)^{-1}$, $b > 0$ stands for stretching and $b < 0$ stands for shrinking of the surface, ζ is a parameter with dimension $(time)^{-1}$ which shows the unsteadiness of the problem. Flow of viscoelastic fluid is driven by this stretching/shrinking movement of the surface in region $y > 0$ with a fixed stagnation point $x = 0$.

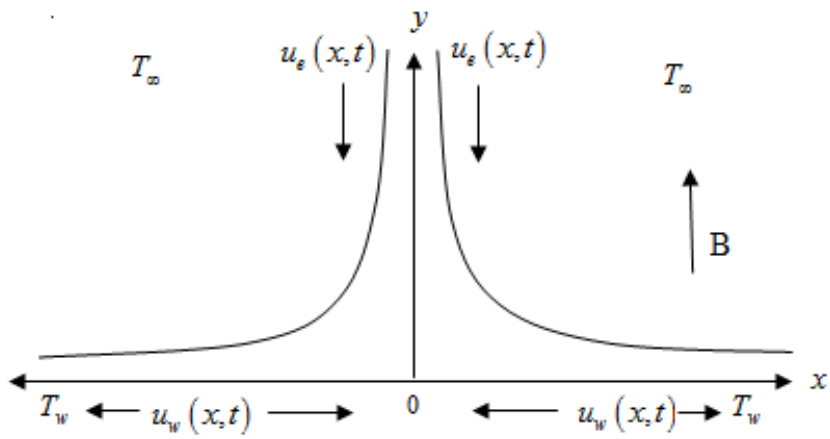

***Figure* 2.1:** Physical configuration of the problem.

A non uniform magnetic field of intensity $B = \dfrac{B_0}{\sqrt{(1-\zeta t)}}$ is applied in transverse direction to flow, where B_0 is the initial strength of magnetic field. It is assumed that magnetic Reynolds number is very small. The flow problem under above considerations is governed by the following boundary layer equations:

Equation of continuity

$$\frac{\partial u}{\partial x} + \frac{\partial v}{\partial y} = 0. \tag{2.1}$$

Equation of motion

$$\frac{\partial u}{\partial t} + u\frac{\partial u}{\partial x} + v\frac{\partial u}{\partial y} = -\frac{1}{\rho}\frac{\partial p}{\partial x} + \nu\frac{\partial^2 u}{\partial y^2} - \beta^*(u^2\frac{\partial^2 u}{\partial x^2} + v^2\frac{\partial^2 u}{\partial y^2} + 2uv\frac{\partial^2 u}{\partial x \partial y}) - \frac{\sigma B^2}{\rho}u - \frac{\nu}{k^*}u. \tag{2.2}$$

Equation of energy

$$\frac{\partial T}{\partial t} + u\frac{\partial T}{\partial x} + v\frac{\partial T}{\partial y} = \frac{\kappa}{\rho C_p}\frac{\partial^2 T}{\partial y^2} + \frac{Q^*}{\rho C_p}(T - T_\infty). \tag{2.3}$$

In above equations, u and v are velocity components in x and y directions respectively, t is the time, p is the pressure, $\beta^*(t) = \beta_0(1-\zeta t)$ is the relaxation time of the *UCM* fluid, σ is the electrical conductivity, ρ is the density, ν is the kinematic viscosity, $k^*(t) = k_0(1-\zeta t)$ is the time dependent permeability of the medium with k_0 being the initial value of permeability coefficient, T is the temperature, κ is the thermal conductivity, C_p is the specific heat at constant pressure, $Q^*(t) = \dfrac{Q_0}{(1-\zeta t)}$ is the time dependent heat generation ($Q^* > 0$) or absorption ($Q^* < 0$) coefficient with Q_0 being the initial value of heat generation/absorption coefficient, T_∞ is the constant temperature of the fluid far away from the surface.

The corresponding boundary conditions are

$$\begin{aligned} t < 0 &: u = 0, v = 0, T = T_\infty \qquad \forall x, y; \\ t \geq 0 &: u = u_w(x,t), v = 0, T = T_w = T_\infty + \frac{T_0}{(1-\zeta t)^{3/2}} \qquad at \quad y = 0 \\ u \to u_e(x,t) &= \frac{ax}{(1-\zeta t)}, T \to T_\infty, \qquad as \quad y \to \infty. \end{aligned} \tag{2.4}$$

Here, T_w is the time dependent temperature of the surface where T_0 is a constant, $u_e(x,t)$ is the free stream velocity where $a > 0$ is a constant for the strength of stagnation with dimension $(time)^{-1}$. The expressions of $u_w, B, \beta^*, k^*, Q^*, T$ and u_e are valid for time $t < \dfrac{1}{\zeta}$.

In the free stream field, the momentum equation (2.2) can be written as

$$\frac{\partial u_e}{\partial t} + u_e \frac{\partial u_e}{\partial x} = -\frac{1}{\rho}\frac{\partial p}{\partial x} - \left(\frac{\sigma B^2}{\rho} + \frac{\nu}{k^*}\right) u_e. \tag{2.5}$$

Using Eq. (2.5) to eliminate the pressure term from Eq. (2.2), we get

$$\frac{\partial u}{\partial t} + u\frac{\partial u}{\partial x} + v\frac{\partial u}{\partial y} = \frac{\partial u_e}{\partial t} + u_e\frac{\partial u_e}{\partial x} + \nu\frac{\partial^2 u}{\partial y^2} - \beta^*\left(u^2\frac{\partial^2 u}{\partial x^2} + v^2\frac{\partial^2 u}{\partial y^2} + 2uv\frac{\partial^2 u}{\partial x \partial y}\right) + \left(\frac{\sigma B^2}{\rho} + \frac{\nu}{k^*}\right)(u_e - u). \tag{2.6}$$

3. Method of Solution

First of all, we introduce the stream function $\psi(x,y)$ defined as

$$u = \frac{\partial \psi}{\partial y} \qquad \text{and} \qquad v = -\frac{\partial \psi}{\partial x}. \tag{3.1}$$

Equation (2.1) is identically satisfied by Eq. (3.1). Also, we introduce following similarity variable and dimensionless variables

$$\eta = y\left(\frac{a}{\nu(1-\zeta t)}\right)^{1/2}, \qquad \psi = x\left(\frac{a\nu}{1-\zeta t}\right)^{1/2} f(\eta), \qquad \theta(\eta) = \frac{T - T_\infty}{T_w - T_\infty}, \tag{3.2}$$

where η is a similarity variable, f and θ are dimensionless stream function and temperature, respectively.

Now using Eq. (3.1) and (3.2) into equations (2.6), (2.3) and (2.4), we get their dimensionless form as follows

$$\left(1 - \beta f^2\right) f''' + 2\beta f f' f'' - \gamma\left(f' + \frac{\eta}{2} f'' - 1\right) - f'^2 + f f'' + (M + K)(1 - f') + 1 = 0,$$

$$\frac{1}{Pr}\theta'' + f\theta' - \frac{\gamma}{2}(3\theta + \eta\theta') + Q\theta = 0, \tag{3.3}$$

where (') represents the differentiation with respect to η.

The corresponding boundary conditions are

$$\begin{aligned} f = 0, f' = \lambda, \theta = 1; &\qquad \text{at} \quad \eta = 0 \\ f' = 1, \theta = 0. &\qquad \text{as} \quad \eta \to \infty. \end{aligned} \tag{3.4}$$

The dimensionless parameters in above equations (3.3) and (3.4) are as follows: $\beta = a\beta_0$ is the Maxwells parameter, $\gamma = \dfrac{\zeta}{a}$ is the unsteadiness parameter, $M = \dfrac{\sigma B_0^2}{a\rho}$ is the Hartmann number, $K = \dfrac{\nu}{ak_0}$ is the permeability parameter, $Pr = \dfrac{\mu C_p}{\kappa}$ is the Prandtl number, $Q = \frac{Q_0}{\rho a C_p}$ is the heat generation/absorption parameter and $\lambda = \dfrac{b}{a}$ is the ratio of the rates of velocity i.e. velocity ratio parameter.

The above system of differential equations (3.3) is coupled and non-linear. We solve it numerically. To solve this system along with boundary conditions (3.4), we use the shooting method. First of all, we convert the above boundary

value problem into a system of initial value problems by taking initial guesses of f'' and θ' at $\eta = 0$. We get the corresponding system of initial value problems as

$$f = f_1, f' = f_2, f'' = f_3, \theta = f_4, \theta' = f_5,$$
$$f''' = \frac{1}{(1-\beta f_1^2)}\{\gamma(f_2 + \frac{\eta}{2}f_3 - 1) + {f_2}^2 - f_1 f_3 - 2\beta f_1 f_2 f_3 - (M+K)(1-f_2) - 1\},$$
$$\theta'' = Pr\{\frac{\gamma}{2}(3f_4 + \eta f_5) - f_1 f_5 - Q f_4\}, \quad (3.5)$$

with the boundary conditions

$$f_1(0) = 0, f_2(0) = \lambda, f_3(0) = c_{01}, f_4(0) = 1, f_5(0) = c_{02}, \quad (3.6)$$

where c_{01} and c_{02} are unknown quantities.

System of differential equations (3.5) along with boundary conditions (3.6) can be solved by using any suitable numerical method. Here we use the Runge-Kutta fourth order method. To solve this system we choose initial guesses of c_{01} and c_{02} and using Runge-Kutta fourth order method the integration is carried out to calculate values of f_2 and f_4 at $\eta \to \infty$ (say η_∞). Here we choose η_∞ suitably finite. These calculated values of $f_2(\eta_\infty)$ and $f_4(\eta_\infty)$ are compared with the given boundary conditions at $\eta \to \infty$ and then by using Runge-Kutta method we find the better approximation for the solution. This process is repeated until we get correct results up to the desired accuracy of 10^{-5}.

The physical quantities of interest, the rate of flow (Skin-friction coefficient C_{f_x}) and the rate of heat transfer (Nusselt number Nu_x) are given as

$${Re_x}^{1/2} C_{f_x} = (1+\beta) f''(0) \qquad and \qquad Nu_x = -{Re_x}^{1/2}\theta'(0), \quad (3.7)$$

where $Re_x = \frac{x u_w(x)}{\nu}$ is the local Reynolds number.

4. Results and Discussion

There are different parameters occur in the problem those affect the flow and heat transfer characteristics of viscoelastic fluid which passes through a porous medium over a stretching/shrinking surface. The effect of physical parameters Maxwells parameter (β), unsteadiness parameter (γ), Hartmann number (M), Permeability parameter (K), Prandtl number (Pr), Heat generation/absorption parameter (Q) and velocity ratio parameter (λ) on the velocity and temperature of the Maxwell fluid are studied numerically and shown through graphs. Also the effect of these parameters on skin friction coefficient (C_{f_x}) and Nusselt number (Nu_x) are discussed through tables. For the validation of the method used in the present study, we compare the results with available results [Bhattacharyya [2], Wang [18]] corresponding to the skin-friction coefficient in the absence of Maxwell parameter, unsteadiness parameter, magnetic field and porosity of the medium. We can depict from Table 4.1 that our results have good agreement with those previous studies.

***Table* 4.1: Comparison of numerical values of $f''(0)$.**

λ	Present study		Wang [18]		Bhattacharya [2]	
	1st solution	2nd solution	1st solution	2nd solution	1st solution	2nd solution
-1.10	1.186680	0.049229				
-1.15	1.08223117	0.11670214	1.08223	0.116702	1.0822316	0.1167023
-1.20	0.93247335	0.23364973			0.9324728	0.2336491
-1.2465	0.58428168	0.55429618	0.55430		0.5842915	0.5542856

The effect of Hartmann number on velocity is drawn in Fig. 4.1. It is depicted that velocity profile decreases with the increasing values of Hartmann number when velocity ratio parameter i.e. $\lambda > 1$ while it increases with the increasing values of Hartmann number when $\lambda < 1$. Fig. 4.2 shows the effect of permeability parameter on velocity profile and it is clear that velocity profile decreases with the increment of permeability parameter when $\lambda > 1$ while it increases with the increment of permeability parameter when $\lambda < 1$.

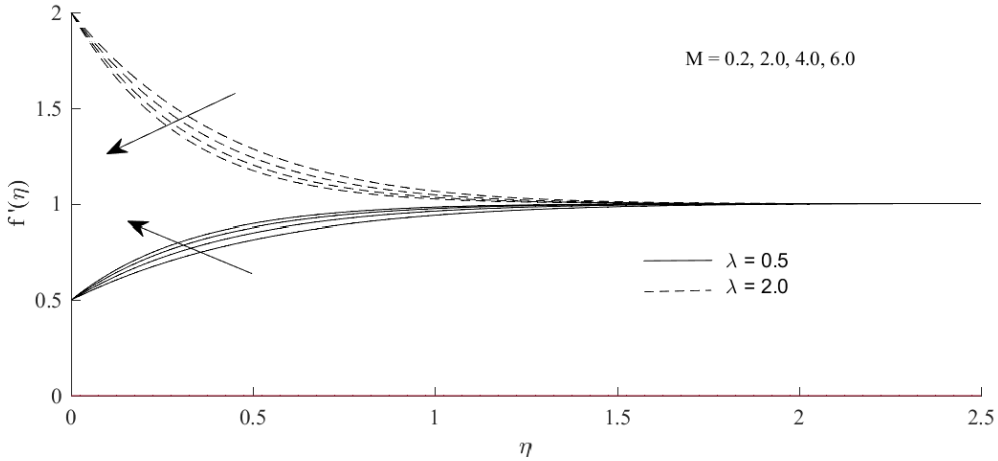

***Figure* 4.1:** Velocity profile for Hartmann number.

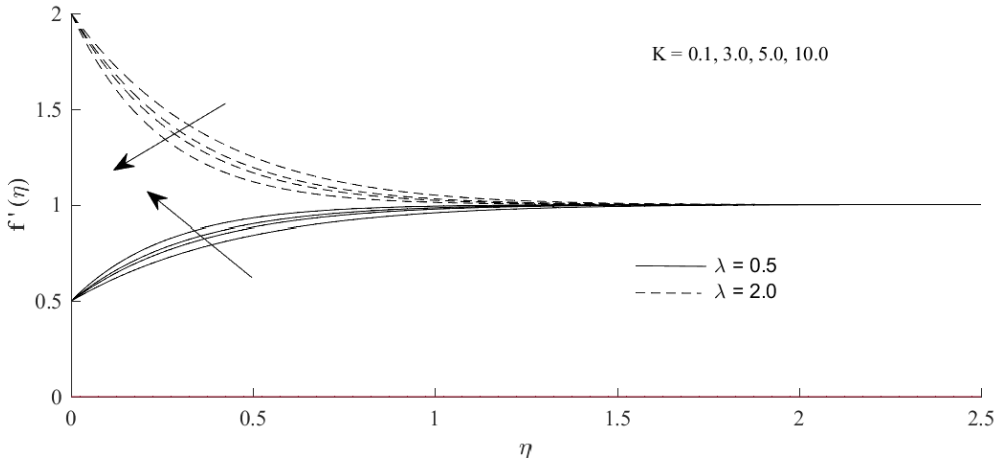

***Figure* 4.2:** Velocity profile for permeability parameter.

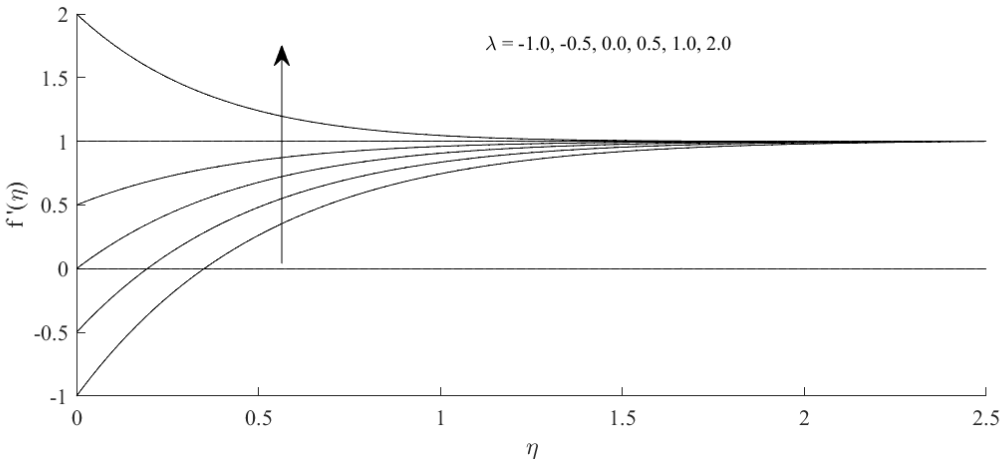

***Figure* 4.3a:** Velocity profile for velocity ratio parameter.

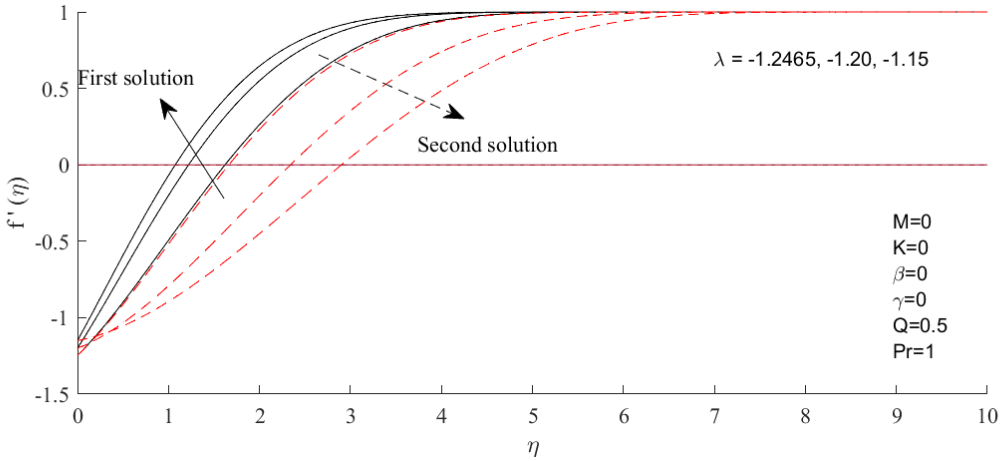

***Figure* 4.3b:** Dual velocity profiles for velocity ratio parameter.

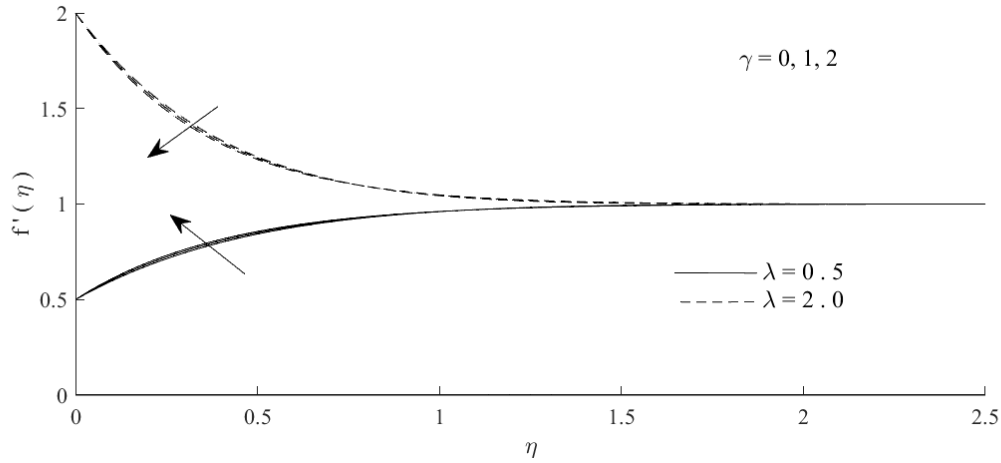

***Figure* 4.4a:** Velocity profile for unsteadiness parameter.

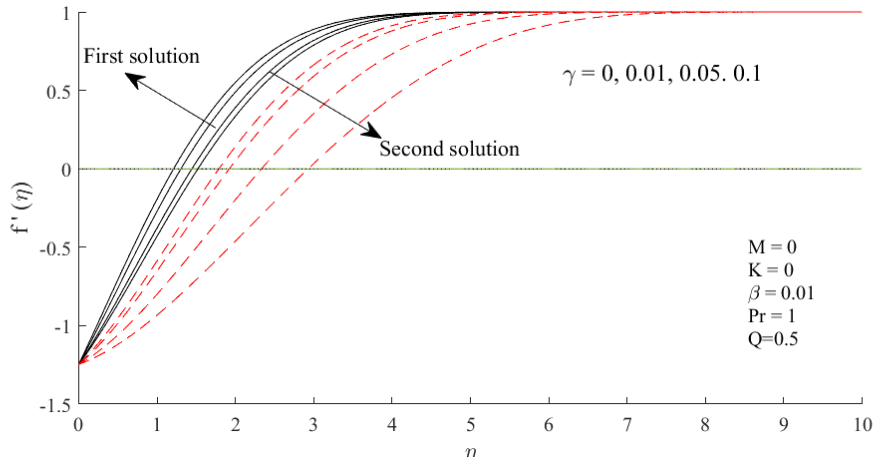

***Figure* 4.4b:** Dual Velocity profiles for unsteadiness parameter when $\lambda = -1.2465$.

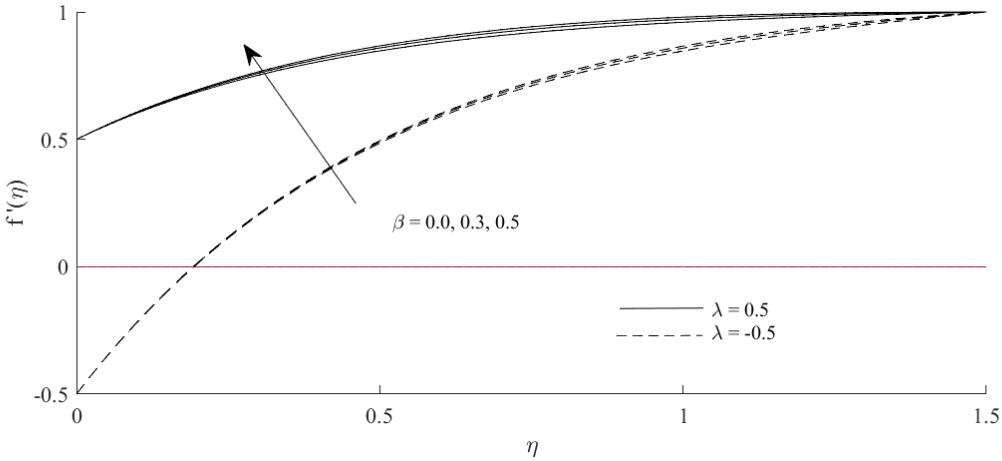

***Figure* 4.5:** Velocity profile for Maxwell parameter.

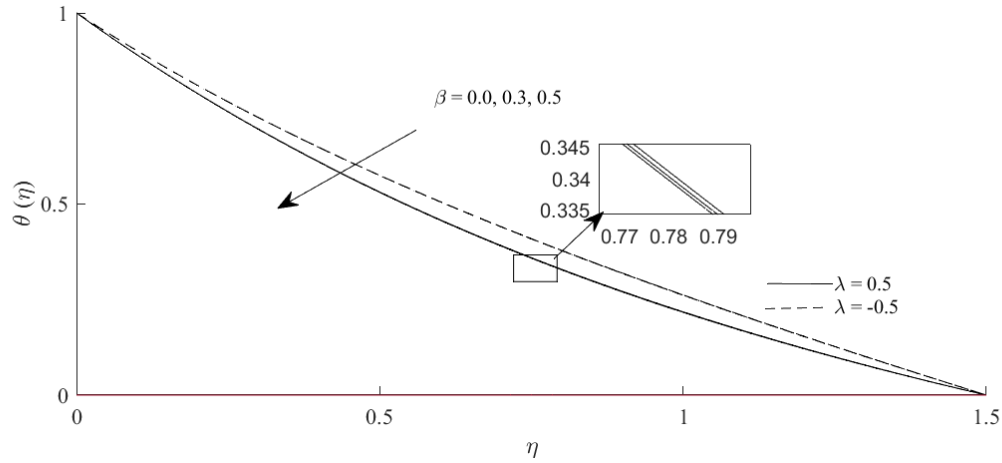

***Figure* 4.6:** Temperature profile for Maxwell parameter.

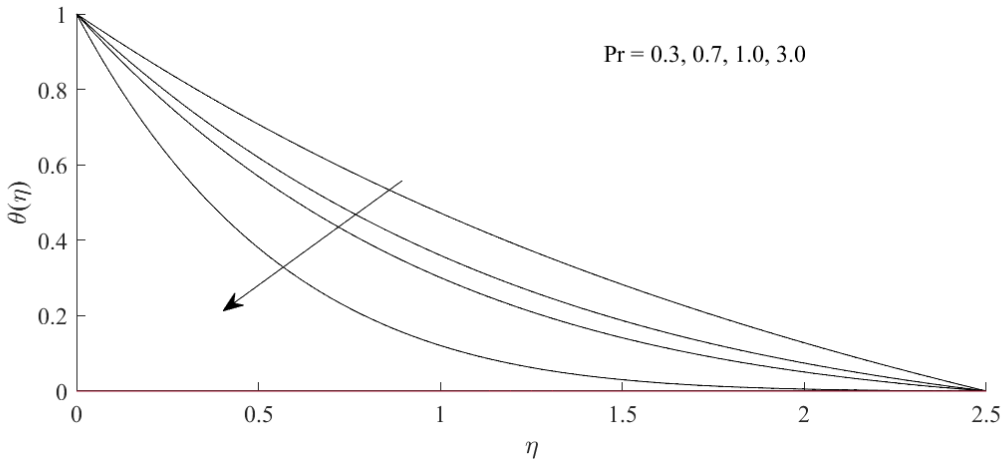

***Figure* 4.7:** Temperature profile for Prandtl number.

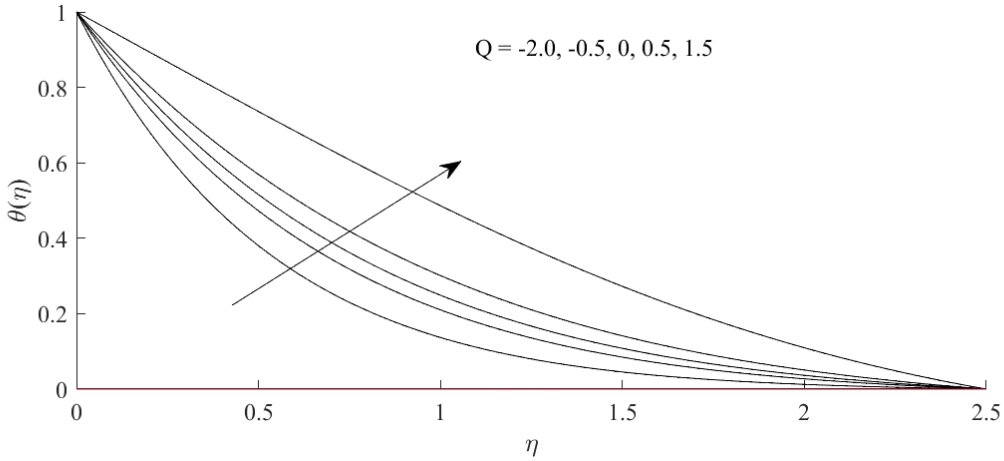

***Figure* 4.8:** Temperature profile for Heat source/sink parameter.

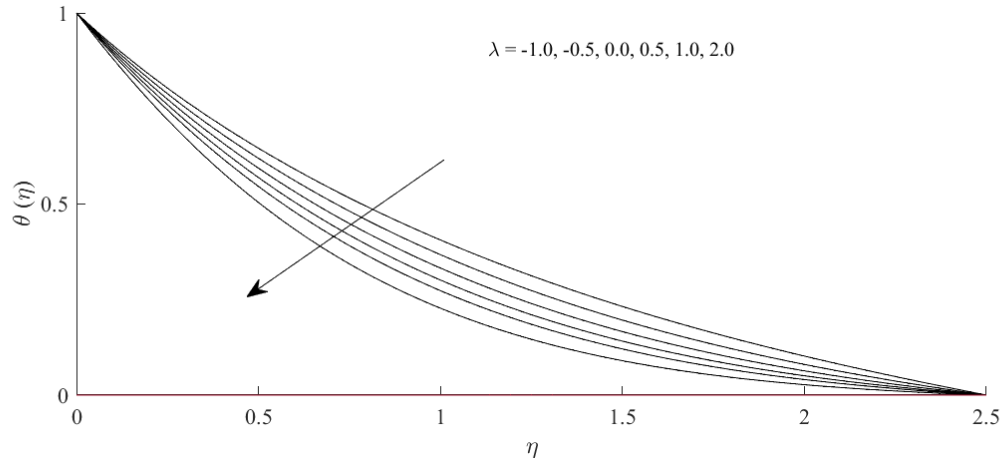

***Figure* 4.9a:** Temperature profile for velocity ratio parameter.

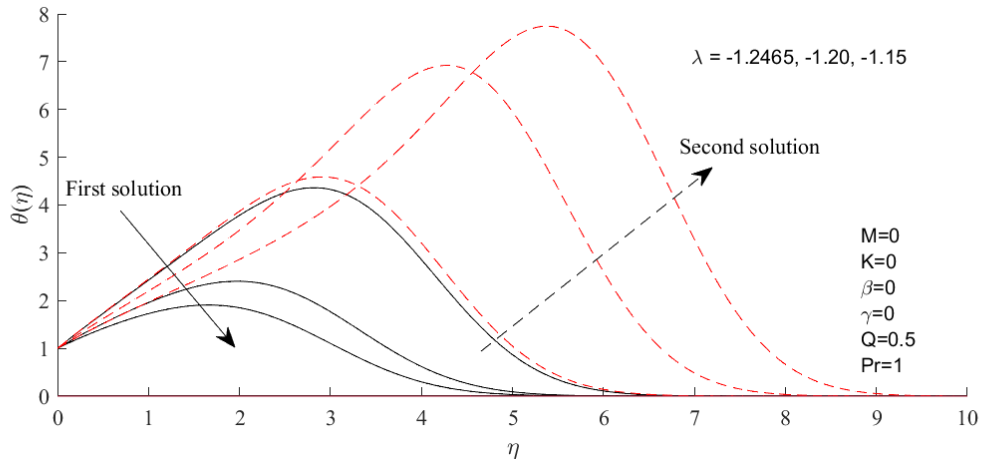

***Figure* 4.9b:** Dual temperature profiles for velocity ratio parameter.

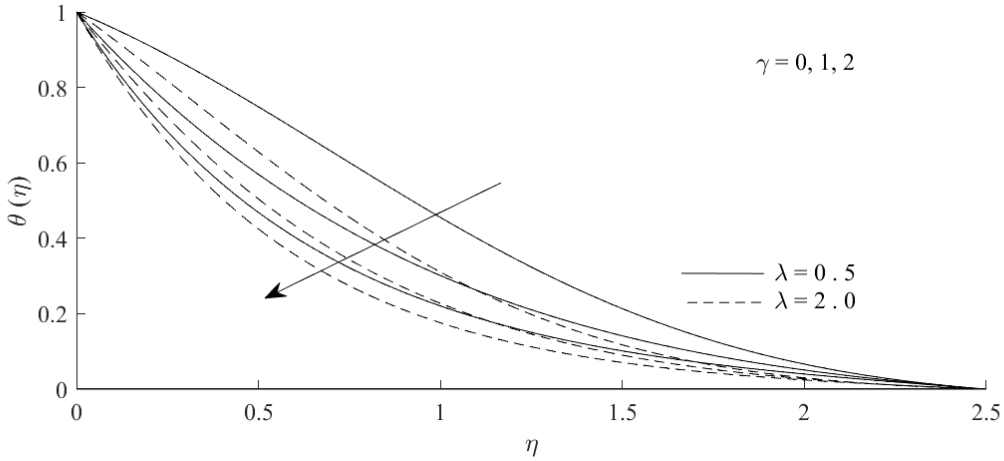

***Figure* 4.10a:** Temperature profile for unsteadiness parameter.

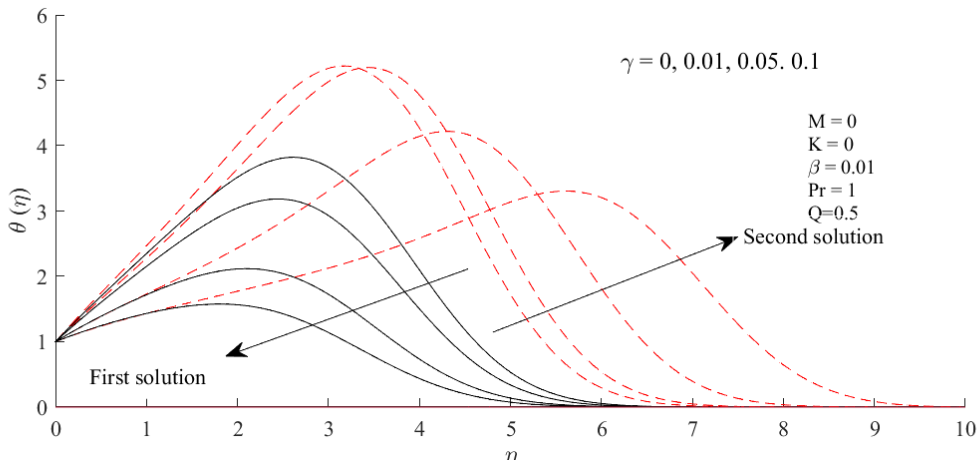

***Figure* 4.10b:** Dual Temperature profiles for unsteadiness parameter when $\lambda = -1.2465$.

Fig.4.3(a) and 4.3(b) show the effect of velocity ratio parameter on velocity profile. Dual solutions are shown in Fig. 4.3(b) and it is clear that f' increases with the increasing values of velocity ratio parameter for the first solution as well as in the unique solution case and f' decreases with the increasing values of velocity ratio parameter for the second solution. From this result, we can also conclude that first solution is stable solution here. The effect of unsteadiness parameter on velocity profile is shown in Fig.4.4(a) and 4.4(b). It is depicted from Fig.4.4(a) that velocity profile decreases with the increasing values of unsteadiness parameter when $\lambda > 1$ while it increases with the increasing values of unsteadiness parameter when $-1 < \lambda < 1$. it is observed that velocity profile increases with the increment of the unsteadiness parameter for unique and first solution case when $\lambda < 1$ but reverse effect is seen in second solution case.

The effect of Maxwell parameter(elastic parameter) is shown in Fig.4.5 and it is clear that whenever elasticity of fluid is increased, velocity profile is also increased for $\lambda = 0.5$ and $\lambda = -0.5$. Fig.4.6 shows the effect of Maxwell parameter on temperature profile and it is depicted that temperature profile decreases with the increasing values of Maxwell parameter. Fig.4.7 shows the effect of Prandtl number on temperature profile and it is depicted that temperature profile decreases with the increasing values of Prandtl number. The effect of heat source/sink parameter on temperature profile is shown in Fig.4.8 and it is clear that whenever this parameter is increased, temperature profile is also increased.

The effects of velocity ratio parameter on temperature profile are demonstrated in Fig. 4.9(a) and 4.9(b). The effects of unsteadiness parameter on temperature profile are demonstrated in Fig. 4.10(a) and 4.10(b). It is depicted

that temperature profile decreases with the increment of velocity ratio parameter and unsteadiness parameter for unique and first solution case while reverse behavior is observed in second solution case.

***Table* 4.2: Numerical values of $f''(0)$ for different values of physical parameters.**

M	K	β	γ	$f''(0)$ when $\lambda = 0.5$	$f''(0)$ when $\lambda = 2.0$
0.2	0.5	0.1	1.0	0.9407251	-2.3188216
2.0	0.5	0.1	1.0	1.155025	-2.6759776
4.0	0.5	0.1	1.0	1.3541066	-3.0250033
2.0	3.0	0.1	1.0	1.3994723	-3.1062487
2.0	0.5	0.0	1.0	1.1458646	-2.6002775
2.0	0.5	0.1	2.0	1.2327104	-2.8078798

***Table* 4.3: Numerical values of $-\theta'(0)$ for different values of physical parameters.**

M	K	β	γ	Pr	Q	$-\theta'(0)$ when λ=0.5	$-\theta'(0)$ when λ=2.0
0.2	0.5	0.1	1.0	1.0	0.5	1.069687	1.255054
2.0	0.5	0.1	1.0	1.0	0.5	1.075574	1.246809
4.0	0.5	0.1	1.0	1.0	0.5	1.0801809	1.239676
2.0	3.0	0.1	1.0	1.0	0.5	1.0811337	1.2381338
2.0	0.5	0.0	1.0	1.0	0.5	1.074943	1.2504742
2.0	0.5	0.1	2.0	1.0	0.5	1.538722	1.6670811
2.0	0.5	0.1	1.0	0.3	0.5	0.653557	0.7125382
2.0	0.5	0.1	1.0	3.0	0.5	1.820257	2.2144121
2.0	0.5	0.1	1.0	1.0	-1.5	1.761971	1.8897677
2.0	0.5	0.1	1.0	1.0	1.5	0.530655	0.7630167

Tables 4.2 and 4.3 display the variation in skin friction coefficient and Nusselt number, respectively, with respect to different parameters. From our observations we find out that skin friction coefficient decreases as velocity ratio parameter increases while reverse effect is seen in the case of Nusselt number. It can be clearly seen that skin friction coefficient increases with an increment of Hartmann number, permeability parameter, Maxwell parameter or unsteadiness parameter when $\lambda = 0.5$ while reverse effect is noticed when $\lambda = 2$. Table 4.3 also reveals that Nusselt number increases as the Maxwell parameter, Hartmann number or permeability parameter increases when $\lambda = 0.5$ while reverse effect is observed when $\lambda = 2$. Nusselt number increases with an increment of Prandtl number or unsteadiness parameter while decreases with an increment of heat source/sink parameter.

5. Conclusions

In this paper the upper-convected Maxwell model is considered to formulate the problem of unsteady stagnation point flow of viscoelastic fluid through a porous medium over a stretching/shrinking surface. Besides it, we also consider magnetic effect in the presence of time dependent heat source/sink. A numerical method named Runge-Kutta fourth order method is applied to solve the system of differential equations with the help of shooting technique. The following conclusions are made

(i) The velocity profile decreases with the increasing values of Hartmann number, unsteadiness parameter or permeability parameter when $\lambda > 1$ while opposite behavior is observed when $\lambda < 1$.

(ii) It is observed that when velocity ratio parameter is less than 1 then velocity within the boundary layer increases up to value 1 but when velocity ratio parameter is greater than 1 then velocity within the boundary layer decreases up to the value 1. This behavior is responsible for the reversible effects of other physical parameter on velocity profile whenever velocity ratio parameter is less than 1.

(iii) Velocity profile increases with the increasing values of Maxwell parameter while temperature profile decreases.

(iv) The temperature profile increases as we make an increment in heat source/sink parameter while an opposite behavior is observed with velocity ratio parameter or unsteadiness parameter.
(v) Skin friction coefficient decreases as velocity ratio parameter increases while reverse effect is seen in the case of Nusselt number.
(vi) Skin friction coefficient increases with an increment of Hartmann number, permeability parameter, Maxwell parameter or unsteadiness parameter when $\lambda = 0.5$ while reverse effect is noticed when $\lambda = 2$.
(vii) Nusselt number increases as the Maxwell parameter, Hartmann number or permeability parameter increases when $\lambda = 0.5$ while reverse effect is observed when $\lambda = 2$.

Acknowledgement. The authors are very much thankful to the Editor and Referee for their valuable suggestions to bring the manuscript in its present form.

References

[1] T. Anwar, P. Kumam and W. Watthayu, Influence of ramped wall temperature and ramped wall velocity on unsteady magnetohydrodynamic convective Maxwell fluid flow, *Symmetry*, **12** (2020), 392.
[2] K. Bhattacharyya, Dual solutions in unsteady stagnation-point flow over a shrinking sheet, *Chinese Physics Letter*, **28**(8) (2011), paper 084702(1-4). **Doi:10.1088/0256-307X/28/8/084702**
[3] H. Chen, H. Liang, F. Wang and M. Shen, Unsteady MHD stagnation-point flow toward a shrinking sheet with thermal radiation and slip effects, *Heat Transfer-Asian Research*, **45**(8) (2016), 730-745.
[4] L.J. Crane, Flow past a stretching plate, *J. Appl. Math. Phys. (ZAMP)*, **21** (1970), 645-647.
[5] T. Hayat, M. Awais, M. Qasim and A. A. Hendi, Effects of mass transfer on the stagnation point flow of an upper-convected Maxwell (UCM) fluid, *Int. J. Heat Mass Transfer*, **54** (2011), 37773782.
[6] M. Madhua, N. Kishana and A. J. Chamkha, Unsteady flow of a Maxwell nanofluid over a stretching surface in the presence of magnetohydrodynamic and thermal radiation effects, *Propulsion and Power Research*, **6**(1) (2017), 3140.
[7] T. R. Mahapatra and A. S. Gupta, Heat transfer in stagnation-point flow towards a stretching sheet, *Heat and Mass Transfer*, **38**(6) (2002), 517521.
[8] S. Mukhopadhyay and K. Bhattacharyya, Unsteady flow of a Maxwell fluid over a stretching surface in presence of chemical reaction, *Journal of the Egyptian Mathematical Society*, **20**(3) (2012), 229234.
[9] S. Mukhopadhyay, Heat Transfer Analysis of the Unsteady Flow of a Maxwell Fluid over a Stretching Surface in the Presence of a Heat Source/Sink. *Chinese Physics Letter*, **29**(5) (2012), paper 054703(1-4). **Doi:10.1088/0256-307X/29/5/054703**
[10] W. Na, N. A. Shah, I. Tlili and I. Siddique, Maxwell fluid flow between vertical plates with damped shear and thermal flux: Free convection, *Chin. J. Phys.*, **65** (2020), 367376.
[11] R. Nazar, N. Amin, D. Filip and I. Pop, Unsteady boundary layer flow in the region of the stagnation point on the stretching sheet, *Int. J. Eng. Sci.*, **42** (2004), 1241-1253.
[12] G. K. Ramesh, B. J. Gireesha, T. Hayat and A. Alsaedi, Stagnation point flow of Maxwell fluid towards a permeable surface in the presence of nanoparticles, *Alexandria Engineering Journal*, **55**(2016), 857865.
[13] K. Sadeghy, H. Hajibeygi and S. M. Taghavi, Stagnation-point flow of upper-convected Maxwell fluids, *International Journal of Non-Linear Mechanics*, **41**(10)(2006), 1242-1247.
[14] M. Sajid, I. Ahmad, T. Hayat and M. Ayub, Unsteady flow and heat transfer of a second grade fluid over a stretching sheet, *Commun. Nonlinear Sci. Numer. Simul.*, **14** (2009), 96108.
[15] A. Shahid, The effectiveness of mass transfer in the MHD Upper-Convected Maxwell fluid flow on a stretched porous sheet near stagnation point: A Numerical Investigation, *Inventions*, **5** (2020), 64.
[16] S. A. Shehzad, F. Mabood, A. Rauf and I. Tlili, Forced convective Maxwell fluid flow through rotating disk under the thermophoretic particles motion, *Int. Commun. Heat Mass Transf.*, **116** (2020), 104693.
[17] C. Y. Wang, Liquid film on an unsteady stretching surface, *Quarterly of Applied Mathematics*, **48** (1990), 601-610.
[18] C. Y. Wang, Stagnation flow towards a shrinking sheet, *International Journal of Non-Linear Mechanics*, **43** (5)(2008), 377-382.
[19] Z. A. Zaidi and S. T. Mohyud-Din, Effect of joule heating and MHD in the presence of convective boundary condition for upper convected Maxwell fluid through wall jet, *J. Mol. Liq.*, **230** (2017), 230234.